THE INFLUENCE OF SAMPLE PREPARATION, SOAK TIME, AND HEATING RATE ON MEASURED RECRYSTALLIZATION OF DEFORMED POLYCRYSTALLINE NIOBIUM*

Z. L. Thune[†], T. R. Bieler[‡], Michigan State University, East Lansing, MI, USA

Abstract

Improving accelerator performance relies on consistent production of high-purity niobium superconducting radio-frequency (SRF) cavities. Current production uses an 800°C 3 hr heat treatment, but 900-1000 °C can improve cavity performance via recrystallization (Rx) and grain growth. As Rx is thermally activated, increasing the temperature and/or the heating rate could facilitate a reduction in geometrically necessary dislocation (GND) density that is associated with the degradation of cavity performance via trapped magnetic flux. Recent work shows that increasing the annealing temperature increased the Rx fraction in cold-rolled polycrystalline niobium. However, the influence of heating rate on the extent of Rx was minimal with a 3 hr soak time. To further assess the influence of heating rate on measured Rx, as well as the effects of sample preparation, electron backscatter diffraction (EBSD) was used to quantify the extent of Rx on samples annealed at a single temperature with different soak times. Comparing samples with different surface preparation shows that removing pinned grain boundaries on the free surface reveals a much larger grain size below the surface.

INTRODUCTION

Improving accelerator performance requires production of niobium superconducting radiofrequency (SRF) cavities with consistent performance. Performance inconsistency may arise from the known variability in microstructures in the as-received Nb polycrystalline sheet. This, as well as locally different strain paths during forming in different parts of the half-cell cause spatially variable dislocation arrangement. Post-cavity formation, the heat treatment used to remove hydrogen causes non-homogeneous rearrangement or removal of dislocations by recovery (Rv) and recrystallization (Rx).

Recovery results in removal of most of the dislocations, but the remaining geometrically necessary dislocations (GNDs) associated with the lattice curvature caused by forming are rearranged into low-angle grain boundaries (LAGBs), which are known to trap magnetic flux [1]. LAGBs are very stable, and not easily removed. Recrystallization, also driven by removing dislocation content, occurs when high-angle grain boundaries (HAGBs) sweep through the material, leaving a nearly perfect crystal in their wake with no GNDs [2], and hence, no LAGBs that trap magnetic flux. As Rx proceeds, grain growth occurs driven by reducing grain boundary area, so HAGBs could sweep through the same volume multiple times.

Furthermore, Rv removes stored strain energy (high dislocation density) that also reduces the driving force for Rx that is necessary to remove LAGBs.

Hence, we hypothesize that the standard 3 hr 800 °C heat treatment facilitates Rv more than Rx, so increasing the holding temperature and/or heating rate should result in more complete Rx that removes the GNDs that degrade cavity performance. Higher temperature anneals between 900 and 1000 °C more effectively remove magnetic flux pinning centers [3, 4], increasing the cavity performance, but at the expense of the strength, as these anneals result in significant grain growth from about 50 to 200 μm in diameter, but the extent of Rx was quite different in samples with different strain path history [5].

Therefore, an ideal heat treatment should exist where Rx occurs nearly completely but is stopped before grains grow significantly. As Rx temperatures are higher than Rv temperatures, it is likely that a hotter but shorter heat treatment may enable Rx without too much grain growth, such that an optimal microstructure can be obtained. Also, a higher heating rate may enable reaching the Rx temperature sooner, so that less Rv occurs. It is likely that this optimal condition will depend on the starting microstructure in the sheet before the cavity is even formed [6].

The present work builds upon prior work [5] to examine the effect of soak time at 940 °C on the extent of Rx after a standard (slow) and a fast heating rate were examined to determine how much the heating rate and soak time influence the Rx process. As the specimen preparation methods varied in these prior investigations and may have affected the measured results, this paper focuses on the effects of methodology on measuring the Rx fraction. Also, the limitations of the analytical method were examined by comparing scans made with the standard Hough transform indexing methods and a spherical indexing method [7] to determine if spatial and angular resolution affected the assessment of the Rx fraction.

EXPERIMENTAL DETAILS

To investigate the effects of the deformation path on microstructure evolution during heat treatment, a proxy for cavities was chosen, by imposing about 30% rolling reduction in coupons in two different directions: the original rolling direction, and the original transverse direction (perpendicular to the rolling direction) [5]. These coupons were carefully polished before heat treatment at different temperatures and heating rates with the same soak time of 3 hr. Samples were heated in evacuated fused quartz ampules to protect the polished characterized surface from oxidation. To assess the fraction Rx in each sample, the same locations on the same surfaces were examined to compare with

† thunezac@msu.edu
‡ bieler@msu.edu

SRF Technology

Nb material

the prior non-heat treated microstructure. The lattice curvature, identified from EBSD mapping, was analytically converted into a GND density (based upon several assumptions [5, 8]). While the recrystallized grains had a very low GND density (essentially the floor of the detection limit for the parameters used), the recovered grains maintained a high GND density. Despite inherent assumptions in the analytical model, systematic comparisons showed that the two different deformation paths resulted in Rx grain fraction that differed by a factor of two at 940 °C.

Cavity Proxy Coupon Samples

The material used for coupon samples was from a ~4 mm thick sheet of Tokyo Denkai niobium used to fabricate an end-cap for a low beta cavity for the Facility for Rare Isotope Beams. The material had a RRR of ~350 and an impurity content of ~0.008 wt% Ta; < 0.0005 wt% H; and < 0.001 wt% W, Ti, Fe, Si, Mo, Ni, Zr, Hf, O, N, and C. Pieces were rolled at ~23 °C to ~30% reduction in three passes without lubrication in a laboratory rolling mill with 100 mm rolls to generate equivalent strains similar to equivalent strains in the iris and equator regions of a formed 1.3 GHz cavity. The influence of the rolling direction on microstructural change during heat treatment was examined by rolling one piece in the original rolling direction (RD), and two pieces in the transverse direction (TD) [5]. Fig. 1 illustrates the locations and shapes of samples used for both the 3 hr Rx study (RD Piece and TD Piece 1) [5] and the 10 or 20 min 940 °C samples (RD Piece and TD Piece 2) presented in this work.

As-received (AR) material adjacent to the rolled pieces was characterized to provide a basis for comparison between the cold-rolled (CR) and heat treated (HT) samples. Rectangular coupon samples were cut from the CR pieces using wire electrical discharge machining (EDM); 10 from each of the TD pieces and 24 from the RD piece. To
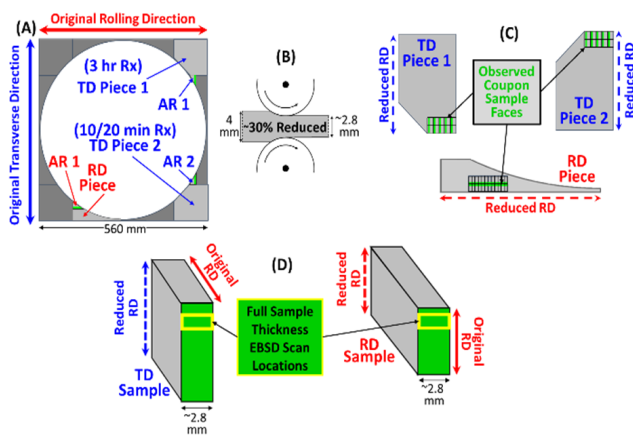

Figure 1: Coupon sample preparation scheme. (A) Pieces taken from the corners of a Nb sheet (RRR ~350) used for low-β end-caps (for MSU FRIB). (B) Cold-rolled to ~30% reduction along the original RD or along the original TD. (C) Samples from each cold-rolled piece ex-tracted using wire EDM. (D) Standard BCP solution to remove the EDM re-cast surface prior to heat treatment and EBSD analysis.

minimize the influence of sample to sample orientation variations, the same surface (labeled green) was observed in the same location in each coupon.

Sample Surface Preparation & Heat Treatment

Different groups of samples were polished using different methods. To remove the EDM re-cast surfaces, all samples were first given a buffered chemical polish (BCP) using a solution of HF, HNO$_3$, and H$_3$PO$_4$.

3 hr Rx Sample Preparation The AR and TD samples were mechanically polished using 15-0.1 µm diamond suspensions before a 0.04 µm colloidal silica vibratory lap final polish [5]. The RD samples were electropolished (EP) in a 9:1 solution of H$_2$SO$_4$ and HF, where the sample (anode) was held ~2 cm from a pure aluminum cathode and the potential was held constant at 16 V for ~8 min. The acid solution was kept below ~25 °C by intermittently cooling the bath container via partial submersion in methanol chilled with liquid nitrogen. After polishing, EBSD maps were made in a specific location on each of the AR, cold rolled TD, and cold rolled RD samples.

3 hr Rx Heat Treatments All RD and TD samples were individually encapsulated in fused quartz ampules under a ~1×10^{-3} Torr vacuum, and then heat treated in a Thermo Scientific Lindberg/Blue M air furnace. Half of the samples were placed in the furnace programmed for a standard heating rate of ~5 °C/min (~3 hr to reach the 800, 900, 940, 975, or 1000 °C soak temperature), and the other half were placed in the furnace when the temperature reached ~90% of the target temperature for a *fast* heating rate ≤ ~50 °C/min (~20 min to reach the assigned soak temperature). To minimize the variation in thermal history, all samples with the same soak temperature were completed in a single furnace run.

10 or 20 min 940 °C Rx Heat Treatments After the standard BCP, RD and TD samples were encapsulated in pairs within fused quartz ampules under a ~1×10^{-3} Torr vacuum, and then heat treated in a Thermo Scientific Lindberg/Blue M air furnace. Half of the ampules were placed in the furnace at ~25 °C programmed for a standard heating rate of ~5 °C/min (~3 hr to reach the soak temperature), and the other half were placed in the furnace when the temperature reached ~90% of the target temperature (~846 °C) for a *fast* heating rate of ~46 °C/min (~20 min to reach the soak temperature). The sample sets were heat treated at 940 °C for either a 10 or 20 min soak and were electropolished *after* heat treatment.

10 or 20 min Rx Sample Preparation Aside from the standard BCP, these samples were not mechanically polished or electropolished prior to encapsulation and heat treatment. The RD and TD samples were encapsulated in pairs within the same ampules, and then heat treated in the same way as described above. After heat treatment, the TD samples were first electropolished as described above without a chilled solution, and then at 10 V without a chilled solution for ~8 min to achieve an acceptable

surface for EBSD. The RD samples were electropolished without the chilled solution at 10 V for ~8 min. The RD samples were electropolished a second time after EBSD to investigate the influence of surface preparation and material removal on the extent of Rx.

Table 1 summarizes similarities and differences in the sample preparation and heat treatment history for the 3 hr soak at different temperatures, and the 10 or 20 min 940 °C samples.

Table 1: Sample Surface Preparation History

Process Sequence	AR	3 hr	10 or 20 min
EDM + BCP	TD + RD	TD + RD	TD + RD
Mech. Polish	TD + RD	TD	
16 V EP 8min		RD	
Vacuum HT		TD + RD	TD + RD
15 V EP 8min		RD-900 (S)	TD
10 V EP 8min			TD + RD
10 V EP 8min			RD

EBSD Data Collection and Analysis

Each coupon was characterized using 1000 μm wide EBSD scans of the full cross-section thickness (~2.8 mm). The EBSD scans were acquired using a Zeiss Auriga XB Crossbeam Field Emission Gun Scanning Electron Microscope with an EDAX/AMETEK Electron Backscatter Detector and TSL-OIM data collection software. Imaging conditions were 9 mm working distance, 40x magnification, 22 kV beam voltage, and a 2 μm EBSD step size.

The EBSD datasets were analyzed using EDAX/AMETEK OIM Analysis software version 8.6. The orientations in each scan were rotated 90° about the y-axis so the crystal orientations, pole figures, and orientation maps are represented with respect to the sheet normal direction. The datasets were filtered to exclude points with a confidence index (CI) less than 0.1; the majority of excluded points were clustered in regions with low pattern/image quality (IQ). The 3 hr heat treated samples were scanned before and after heat treatment within ~50 μm of the same location on the sample surface, but the RD-900(S) did not provide good EBSD patterns after the heat treatment, so it was electropolished a second time. The 10 and 20 min samples at 940 °C were scanned after electropolishing, and to further assess the effect of proximity of the original surface to the scanned surface, the RD samples were electropolished a second time.

To assess the effect of spatial resolution and angular resolution on assessing the fraction recrystallized, two 50×50 μm scans with a 0.5 μm step size on the TD and RD 3 hr 900 °C fast heating rate samples were made with the patterns stored for implementation of spherical harmonic indexing [8] to be compared to the traditional Hough indexing.

SRF Technology

Nb material

RESULTS AND DISCUSSION

As Rx grains form by the migration of HAGBs through deformed material, leaving a nearly defect-free crystal in their wake, the Rx fraction can be quantified by measuring the lattice curvature, which is a metric of the GND content, and hence, deformation. By assessing the lattice curvature at each pixel, a theoretical GND density can be extracted based upon [8] using the OIM Analysis software. Figure 2 plots the distribution of GND density for each of the 3 hr heat treated samples at different soak temperatures (solid lines are the fast (F) and dashed are the standard (S) heating rates). The AR material (solid black line) has a GND density peak at about $3 \times 10^{12}/m^2$, while the CR material (dotted black line) has a GND density peak at about $30 \times 10^{12}/m^2$. With increasing temperature, the amplitude of the deformed/recovered peak decreases with the formation of Rx grains that have a GND peak at about $10^{12}/m^2$, and its amplitude increases with the Rx fraction. The ratio of the left peak area (up to $10 \times 10^{12}/m^2$) over the entire area provides the Rx fraction. The RD Rx fraction is greater than the TD at all temperatures for the 3 hr heat treatments.
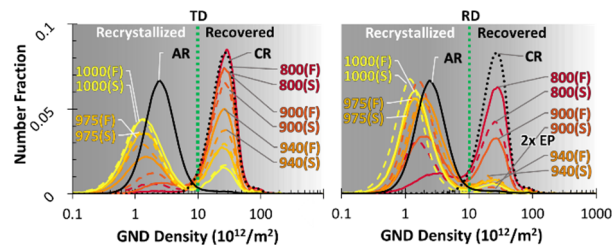

Figure 2: GND density distribution for each sample of the 3 hr Rx study shows a bimodal distribution associated with recrystallized grains (left peak in either plot) and recovered grains (right peak in either plot).

The Rx fraction of the 940 °C 10 or 20 min and 3 hr soak samples is illustrated as a colored bar overlaid on maps with black grain boundaries in Fig. 3 that show which grains are recrystallized (white) and which are recovered (gray). The maps reveal the variations in grain size between the 10 or 20 min TD and RD samples after the first EP, indicating the inconsistent removal of material due to necessary additional EP rounds for EBSD. The fact that the Rx fraction is higher for the 10 and 20 min 940 °C (blue, green) than the 3 hr (red) TD samples, with similar fractions for the RD samples, needs an explanation, as this is inconsistent with established understanding of Rx [2].

Consequently, a second EP was done on the RD samples to reassess the microstructure. With removal of more material, both the grain size and the Rx fraction increased (Figs. 4-6).

This study shows that the care taken to observe the same surface before and after heat treatment led to the observation of a significant surface artifact. It is well known that annealing in vacuum will enable surface diffusion to minimize the interfacial energy where grain boundaries meet the surface, resulting in grain boundary grooving [9]. The grooves can pin the grain boundary, making it more

21th Int. Conf. RF Supercond.

ISBN: 978–3–95450–234–9

SRF2023, Grand Rapids, MI, USA

ISSN: 2673–5504

JACoW Publishing

doi:10.18429/JACoW-SRF2023-WEPWB116

difficult for a grain boundary on the free surface to move. Hence, measurement of the Rx fraction without the influence of surface energy requires removal of surface grains.

This surface pinning effect also explains an outlier in the data in Fig. 2. Comparing the fast (solid) and standard heat treating rate (dashed) curves for each temperature, they are close to each other in all cases except the RD 900 °C standard heating rate sample (*RD-900 (S)*), which has a much lower Rv peak than the fast heating rate sample (*RD-900(F)*) at the same temperature. The standard heating rate sample could not be indexed after the heat treatment due to surface contamination, so it was electropolished a second time to enable it to be measured and this removed enough

of the pinned surface grains to increase the visible fraction of Rx grains.

This grain boundary pinning effect that hinders Rx is relevant for cavity performance. As the interior surface of the cavity is where the superconducting activity takes place, it is desirable to remove defective grains from the surface. This suggests that sufficient EP *after* the heat treatment to remove 20-50 μm is valuable, and that a light EP would not likely alter the surface pinned microstructure sufficiently. This work also shows that the heating rate does not significantly alter the nature of recrystallization near the surfaces, but it is still unclear whether an advantage would be gained in interior grains and is the subject of future work. Clearly, surface preparation has an enormous influence on quantifying Rx and Rv phenomena, and an excellent degree of surface preparation is needed along with cognizance of the surface grain boundary pinning effect in order to interpret results meaningfully.

Also, an assessment of the EBSD accuracy and resolution shows that the same information is gained with conventional Hough and spherical harmonic indexation (see Appendix).
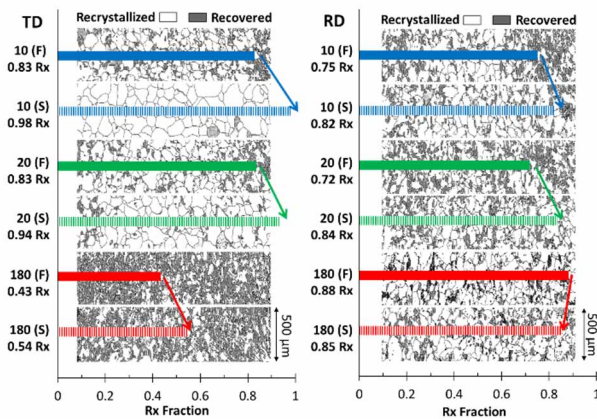

Figure 3: EBSD maps of 940 °C samples colored by the GND density, where recovered grains are gray and recrystallized, white. Surprisingly, the fraction recrystallized in the 10 and 20 min samples is greater than or equivalent to the 3 hr samples, due to removal of the original surface.

Figure 6: The microtexture of RD-10 (F) is nearly unchanged after the second electropolish; however, a majority of the small, recovered grains on the surface have been mostly removed.
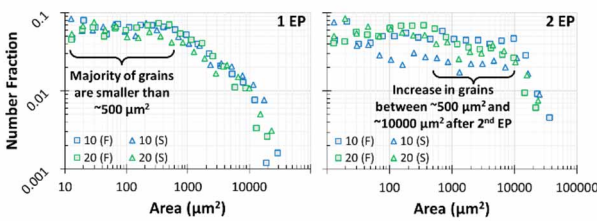

Figure 4: The grain size distributions in the 940 °C RD 10 or 20 min soak samples are similar for both heating rates and annealing times after the first EP (left), but the grains are larger after the second EP (right).
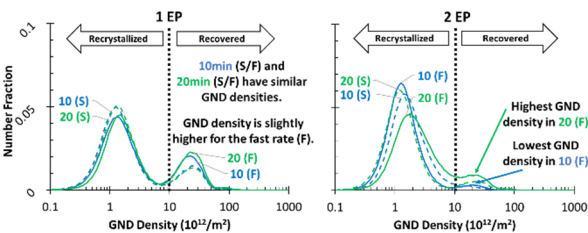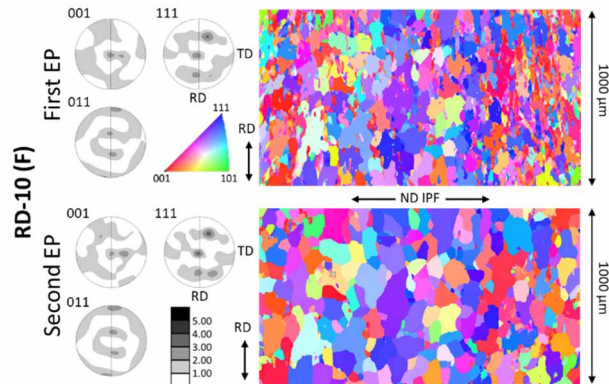

Figure 5: The GND density of the 940 °C RD samples after 10 or 20 min soak times decreased after a second EP (right) indicating a higher Rx fraction due to surface removal.

CONCLUSION

Quantitative measurement of Rx is subject to many systematic errors that can be neglected if all samples are prepared and assessed with the same parameters. Rx on surfaces is strongly retarded by surface grain boundary pinning, indicating that assessing the Rx fraction requires careful experiment design so that surface effects can be managed and understood.

ACKNOWLEDGEMENTS

21ᵗʰ Int. Conf. RF Supercond.

SRF2023, Grand Rapids, MI, USA

JACoW Publishing

ISBN: 978-3-95450-234-9

ISSN: 2673-5504

doi:10.18429/JACoW-SRF2023-WEPWB116

APPENDIX

A comparison of the GND density distribution based on EBSD scans using traditional Hough indexing (black) and spherical harmonic indexing (green) is presented in Fig. 7 for the same $50{\times}50~\mu m^2$ area in each of the fast heating rate 3 hr 900 °C TD and RD samples using both methods [10]. In contrast to the EBSD data presented above, the step size of these scans was 500 nm to ensure highly detailed EBSD patterns for indexing (these scans were also coarsened to assess the effect of spatial resolution). While there are details that are slightly different in the two curves from the same specimen, it is clear that the overall shapes of the two curves are the same, and the Rx fraction (left peak) is lower with the spherical indexing method.

Quantitatively, the Rx fraction is slightly lower (a few %) when using the spherical harmonic method, and a finer spatial resolution shifts the cross over point between the Rx and Rv populations to a higher GND density. Nevertheless, as long as measurements are made in a systematic manner on all samples being compared, the generic EBSD method will provide sufficiently accurate data to be trustworthy, if the surface is carefully prepared to yield a high fraction of high-confidence points.
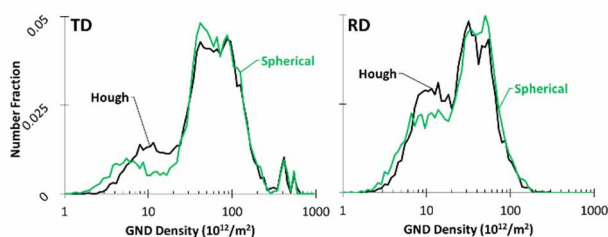

Figure 7: GND density plots for the fast heating rate 3 hr 900 °C TD (left) and RD (right) samples evaluated with both the traditional Hough indexing (black) and the Spherical Harmonic indexing (green). Specific details differ, but they are consistent with each other, indicating that both methods are reliable for assessing the Rx fraction.

REFERENCES

[1] M. Wang *et al.*, "Investigation of the effect of structural defects from hydride precipitation on superconducting properties of high purity SRF cavity Nb using magneto-optical and electron imaging methods", *Supercond. Sci. Technol.*, vol. 35, p. 045001, 2022. doi:10.1088/1361-6668/ac4f6a

[2] R. D. Doherty *et al.*, "Current issues in recrystallization: a review", *Mater. Sci. and Eng.* vol. A238, p. 219, 1997. doi:10.1016/S0921-5093(97)00424-3

[3] S. Posen *et al.*, "The effect of mechanical cold work on the magnetic flux expulsion of niobium", *Accel. Phys.*, 2018. doi:10.48550/arXiv.1804.07207

[4] Z. H. Sung *et al.*, "Evaluation of predictive correlation between flux expulsion and grain growth for superconducting radio frequency cavities", submitted for publication. doi:10.48550/arXiv.2303.14122

[5] Z. L. Thune *et al.*, "The Influence of Strain Path and Heat Treatment Variations on Recrystallization in Cold-Rolled High-Purity Niobium Polycrystals", *IEEE Trans. Appl. Supercond.*, vol. 35, p. 6000504, 2023. doi:10.1109/TASC.2023.3248533

[6] S. Balachandran *et al.*, "Microstructure development in a cold worked SRF Nb sheet undergoing 700°C-900°C/3h heat treatments", presented at SRF'23, Grand Rapids, MI, USA, Jun. 2023, paper MOPMB041, this conference.

[7] W. C. Lenthe *et al.*, "A spherical harmonic transform approach to the indexing of electron back-scattered diffraction patterns," *Ultramicroscopy*, 2019. doi:10.1016/j.ultramic.2019.112841

[8] D. P. Field *et al.*, "Analysis of local orientation gradients in deformed single crystals", *Ultramicroscopy*, vol. 103, p. 33, 2005. doi:10.1016/j.ultramic.2004.11.016

[9] H. Zhang and H. Wong, "Coupled grooving and migration of inclined grain boundaries: Regime I", *Acta Mater.*, vol. 50, p. 1983, 2002. doi:10.1016/S1359-6454(02)00044-7

[10] Z. L. Thune *et al.*, "Investigating Heat-treatment and Strain Path Effects on the Recrystallization of High-Purity Niobium", presented at TMS 2023, San Diego, California, USA, Mar. 2023, paper J-104, this conference.